https://doi.org/10.5194/gmd-2022-258
Preprint. Discussion started: 16 January 2023

Geoscientific Model Development Discussions

An empirical model to calculate snow depth from daily snow water equivalent: SWE2HS 1.0

Johannes Aschauer[1], Adrien Michel[1,2], Tobias Jonas[1], and Christoph Marty[1]

[1]WSL Institute for Snow and Avalanche Research SLF, Davos, Switzerland
[2]School of Architecture, Civil and Environmental Engineering, École Polytechnique Fédérale de Lausanne (EPFL), Lausanne, Switzerland

Correspondence: Johannes Aschauer (johannes.aschauer@slf.ch)

Abstract. Many methods exist to model snow densification in order to calculate the depth of a single snow layer or the depth of the total snow cover from its mass. Most of these densification models need to be tightly integrated with an accumulation and melt model and need many forcing variables at high temporal resolution. However, when trying to model snow depth on climatological timescales, which is often needed for winter tourism related applications, these preconditions can cause barriers. Often, for these types of applications empirical snow models are used. These can estimate snow accumulation and melt based on daily precipitation and temperature data, only. To convert the resultant snow water equivalent time series into snow depth, we developed the empirical model SWE2HS. SWE2HS has been calibrated on a data set derived from a manual observer station network in Switzerland and validated against independent data from automatic weather stations in the European Alps. The model fits the calibration data with root mean squared error (RMSE) of 8.4 cm, coefficient of determination (R^2) of 0.97 and BIAS of 0.2 cm and is able to reach RMSE of 20.5 cm, R^2 of 0.92 and BIAS of 2.5 cm on the validation data. The temporal evolution of the bulk density can be reproduced reasonably well on both data sets. Due to its simplicity, the model can be used as post-processing tool for output of any other snow model that provides daily snow water equivalent output. SWE2HS is available as a Python package which can be easily installed and used.

1 Introduction

Seasonal snow cover is an important variable with regard to ecology, water resource management, and tourism industry. Accordingly, a large range of models of different complexity exist to calculate various properties of the snow cover. Traditionally, snow models were emerging from the hydrological community in order to estimate water resources from snow. Therefore, the focus was set on snow water equivalent (SWE) of the snow cover for the first simple approaches such as the empirical temperature-index models. Over time, more complex models were developed which are capable to calculate snow density, snow temperature profiles (Jordan, 1991), and snow microstructure (Lehning et al., 2002; Vionnet et al., 2012). Most of these more complex, physically based models require a rich set of input parameters such as incoming short and long wave radiation, wind speed, precipitation, and temperature at sub-daily temporal resolution. However, when applying models on longer timescales e.g. for climatological analyses, the required input parameters are often limited with regard to availability and temporal resolution. Accordingly, simpler empirical models are still often used for climatological analyses instead of employing

https://doi.org/10.5194/gmd-2022-258
Preprint. Discussion started: 16 January 2023


Geoscientific Model Development Discussions

more complex physically based models. Empirical models, however, usually do not calculate snow depth (HS), which would be desirable when model output is addressed to stakeholders that usually deal with snow depth rather than snow water equivalent, such as in the winter tourism sector.

Snow depth is the result of SWE and the bulk snow density (ρ), where $\mathrm{SWE} = \mathrm{HS} \cdot \rho$. Snow depth can be measured either manually by reading from snow stakes or automatically with lasers or ultrasonic devices (Kinar and Pomeroy, 2015). While modeling SWE requires the representation of snow mass accumulation and ablation, modeling snow depth needs to address different types of densification processes. These processes involve densification due to stress induced by overlying snow and metamorphic processes that change the size and shape of the snow crystals and thus affect snow density (Anderson, 1976). Metamorphic processes can be either destructive (at constant temperature), constructive (within a temperature gradient) or melt metamorphic (for melt refreeze cycles) (Sommerfeld and LaChapelle, 1970).

All densification models need to initialize the density of a snow layer or of the whole snowpack. Since there is yet no simple method to derive new snow density from a physical snowfall model, in snow models new snow density is either parameterized or kept at a fixed value. Parameterizations are usually made by estimating new snow density as a function of wind speed, temperature and relative humidity and various parameterizations exist (see e.g. Helfricht et al., 2018; Valt et al., 2018). When applied on a daily resolution, the quality of such parameterizations is declining due to unknown timing of a snowfall event during the day and simultaneous occurrence of settling over the course of the day (Meister, 1986).

There exist several methods to model snow densification either per layer or for the entire snowpack which can be roughly classified into three categories. The first category is purely empirical whereby describing the densification dynamic via exponential settling functions. This approach has first been proposed by Martinec (1956) and Martinec (1977) while variations of the method exist (e.g. Dawson et al., 2017; Koch et al., 2019; Essery, 2015; Aili et al., 2019; Brown et al., 2003, 2006). Dawson et al. (2017) for example use a non constant e-folding time of the settling rate based on air temperature with an additive overburden term, Essery (2015) use two different maximum densities for cold and melting snow where the exponential function converges to and Brown et al. (2006) use a maximum density based on snow depth. The second category of snow densification models is the semi-empirical method of Anderson (1976) which employs a two stage compaction due to metamorphism and pressure from overlying snow. The compaction due to stress uses a parameterized viscosity coefficient based on temperature. Settling is enhanced when wet snow in the snowpack occurs. The scheme of Anderson (1976) has been adopted widely and is used in many snow and land surface models such as SNTHERM (Jordan, 1991), AMUNDSEN (Marke et al., 2015; Hanzer et al., 2016; Marke et al., 2018; Warscher et al., 2021), SNOWGRID-CL (Olefs et al., 2020) and CLM5 (van Kampenhout et al., 2017; Lawrence et al., 2019). Due to its need to determine wet snow in the snowpack, the method of Anderson (1976) has to be tightly integrated with a snow melt model. The third and most sophisticated category of snow densification models is using a snow viscosity coefficient which is parameterized based on temperature and/or microstructure of the snow. Snow compaction is then modeled by applying stress due to weight of overlying snow. This requires a complex physical model in order to be able to represent the processes which affect e.g. snow microstructure and is realized by the two physical energy balance models models Crocus (Brun et al., 1992; Vionnet et al., 2012) and SNOWPACK (Bartelt and Lehning, 2002; Lehning et al., 2002).

https://doi.org/10.5194/gmd-2022-258
Preprint. Discussion started: 16 January 2023

Geoscientific Model Development Discussions

To our knowledge, none of the above described densification models can be easily used as a standalone model to transfer daily SWE to snow depth independently of the snow model, while many approaches exist to do the opposite, convert HS into SWE (e.g. Jonas et al., 2009; Winkler et al., 2021; McCreight and Small, 2014; Mizukami and Perica, 2008; Guyennon et al., 2019; Pistocchi, 2016). With new methods being developed to derive SWE from global navigation satellite system (GNSS) signal attenuation (Koch et al., 2019) or by cosmic ray attenuation (Gugerli et al., 2019), it would be even more desirable to be able to model snow depth from the derived SWE data (Capelli et al., 2022). Therefore, we developed a simple empirical snow densification model which uses daily SWE as sole forcing and transforms SWE to HS using exponential settling equations for individual layers inspired by Martinec (1977); Dawson et al. (2017); Koch et al. (2019); Essery (2015). We make an implementation of the model available as a Python package which can be downloaded and installed from the Python packaging index (PyPI).

The remainder of the paper is structured as follows. In Sect. 2 we describe the model as well as the technical implementation. In Sect. 3 we describe the data used for calibration and validation of the model alongside the used calibration methods. In Sect. 4 we show the performance of the calibrated model in alpine snow environments and discuss the scope and limitations of the model in Sect. 5.

2 Density model

The density model SWE2HS calculates snow depth at a daily resolution and is driven by the daily snow water equivalent of the snow cover only. In the following, we use the unit $\mathrm{mm\,w.e.}$ for SWE. The model creates a new layer with a fixed new snow density ρ_{new} for every increase in SWE such that, over time, a snowpack of individual layers builds up. The density of a layer increases exponentially with time towards a time-varying maximum density. The maximum density is starting with an initial value at creation time of the layer and is subsequently increasing towards a higher value based on the overburden a layer has experienced and the occurrence of SWE losses in the snow pack. When SWE decreases, the model removes SWE from the top of the snowpack. The layer number n can thus undergo changes over time based on the number of SWE increases and losses in the snowpack. The model neglects constructive metamorphism, refreezing, and is not able to capture rain-on-snow events which might lead to an increase in SWE but no increase in snow depth.

2.1 Settling mechanisms

The density of a layer at day i is asymptotically converging towards the time-varying ρ_{max} of the layer via the following exponential function:

$$\rho_i = \rho_{max} - (\rho_{max} - \rho_{i-1}) \cdot \exp(\frac{-1}{R}) \tag{1}$$

Where ρ_i is the density of day i and ρ_{i-1} is the layer density of the day before. The settling resistance (e-folding time) R is a model parameter which is optimized in model calibration.

https://doi.org/10.5194/gmd-2022-258
Preprint. Discussion started: 16 January 2023


Geoscientific Model Development Discussions

The maximum density to which the density of a snow layer is converging, ρ_{max} in Eq. 1, is also evolving over time. We model the maximum density of a snow layer based on three assumptions. The first assumption is that snow which experienced a high load is reaching a higher maximum density. The second assumption is that a snow layer is initially dry and that wet snow has a higher maximum density than dry snow. The third assumption is that the the time-varying maximum density cannot decrease. Accordingly, the maximum density of a snow layer undergoes changes during its lifetime and transitions from the model parameters $\rho_{max,init}$ to the model parameter $\rho_{max,end}$. At the time of deposition, the layer has a theoretical maximum snow density of $\rho_{max,init}$. Afterwards, ρ_{max} is increasing towards $\rho_{max,end}$ by two mechanisms as described following.

1. If a layer experiences an overburden $\sigma > 0\,\mathrm{mm}$, its maximum density ρ_{max} is increased linearly with overburden. We calculate σ as a proxy for overburden stress by summing the amount of SWE above a layer and half of the SWE of the layer itself. If the overburden weight is equal or larger than the model parameter σ_{max}, ρ_{max} is capped at $\rho_{max,end}$.

$$\rho^*_{max} = \begin{cases} \frac{(\rho_{max,end} - \rho_{max,init})}{\sigma_{max}} \cdot \sigma + \rho_{max,init} & \text{if } \sigma < \sigma_{max} \\ \rho_{max,end} & \text{if } \sigma \geq \sigma_{max} \end{cases} \tag{2}$$

   If the updated ρ^*_{max} is lower or equal than the value of the day before ($\rho_{max\ i-1}$), the value of the current day ($\rho_{max\ i}$) is not updated which which could otherwise cause a decrease of ρ if the density ρ_{i-1} equals $\rho_{max\ i-1}$ (see Eq. 1).

$$\rho_{max,i} = \begin{cases} \rho^*_{max} & \text{if } \rho^*_{max} \in (\rho_{max\ i-1}, \rho_{max,end}] \\ \rho_{max\ i-1} & \text{if } \rho^*_{max} \leq \rho_{max\ i-1} \end{cases} \tag{3}$$

2. SWE losses are defined by $\mathrm{SWE}_i - \mathrm{SWE}_{i-1} < 0$. Whenever SWE in the snowpack is decreasing, we assume that the snowpack has become wet entirely as we attribute all SWE losses to runoff. In doing so, we neglect losses in SWE due to sublimation. If SWE decreases, we assume melt metamorphism is active and the maximum snow density ρ_{max} of each layer is increased towards $\rho_{max,end}$ by

$$\rho_{max\ i} = \rho_{max,end} - (\rho_{max,end} - \rho_{max\ i-1}) \cdot \exp(-v_{melt}) \tag{4}$$

   Where $\rho_{max\ i}$ is the maximum density of day i, $\rho_{max\ i-1}$ is the maximum density of the day before and v_{melt} is a model parameter for the speed of that transition.

At the end of every time step, the snow depth of the snowpack is calculated by summing up the thickness of all n snow layers in the snowpack as

$$\mathrm{HS} = \sum_{k=1}^{n} \frac{\mathrm{SWE}_k \cdot \rho_{water}}{\rho_k} \tag{5}$$

where ρ_{water} is the density of water with $1000\,\mathrm{kg\,m^{-3}}$ and SWE_k and ρ_k are SWE and density of layer k, respectively. All free model parameters that need to be calibrated are listed in Table 2.

https://doi.org/10.5194/gmd-2022-258
Preprint. Discussion started: 16 January 2023


Geoscientific Model Development Discussions

2.2 Technical implementation

We provide an implementation of the model as a Python package under GNU General Public License v3.0 (GPLv3). One-dimensional station data and two dimensional model grids of SWE time series can be transformed to snow depth with the above described snowpack evolution. Additionally, a step by step processing mode with caching of the model state variables for two dimensional SWE grids of consecutive days is available for operational applications. Python, being a high-level, interpreted general-purpose programming language has been chosen due to its easy-to-read syntax, growing user base and community support for scientific computing and data analysis. Our implementation is using the just-in-time Python compiler *Numba* (Lam et al., 2015) for increasing runtime efficiency. Additionally, it depends on the libraries *NumPy* (Harris et al., 2020) for numerical computations, *Pandas* (Reback et al., 2022) for one dimensional input series, and *xarray* (Hoyer and Hamman, 2017) for multidimensional input grids. The multidimensional, distributed versions of the model can make use of *Dask* (Dask Development Team, 2016) which makes it possible to execute the model in parallel on standalone computers or high performance computing environments. Processing 23 years of the Swiss 1 x 1 km domain (8401 x 365 x 272 pixels) including file IO took ~10 min on a desktop PC (8 cores, Intel Core i7-4790 CPU @ 3.60 GHz, 24 GB RAM). The model implementation can be installed from the official third-party software repository for Python, The Python Package Index (PyPI: https://pypi.org/project/swe2hs, last access: 20.10.2022), the source code of SWE2HS is hosted on a Gitlab instance of the Swiss Federal Institute for Forest, Snow and Landscape Research WSL (https://code.wsl.ch/aschauer/swe2hs, last access: 20.10.2022), and the software version which was used for this publication is archived at https://doi.org/10.5281/zenodo.7228066 (Aschauer, 2022).

3 Model calibration and validation

As for every empirical model, parameters in our density model need to be calibrated. Calibrated parameters may differ depending on the station, snow type and snow climatological setting. Here, we try to find one single generic optimal parameter set which suits most snow climatological conditions in Switzerland and the European Alps in general. We do so by calibration over a data set which covers a large range of different altitudes and climatologic settings in Switzerland (see Section 3.1) and test the found parameters on another independent data set from stations in the European Alps (see Section 3.2). Our model has 6 model parameters which need to be calibrated. Before calibration, we define upper and lower bounds of possible values for each model parameter (see Table 2) and apply the constraints that $\rho_{max,init}$ needs to be smaller than $\rho_{max,end}$ and ρ_{new} needs to be smaller than $\rho_{max,init}$. For parameter calibration, we use the Differential Evolution algorithm which is a stochastic population based method for minimizing nonlinear and non-differentiable continuous space functions as implemented in SciPy (Storn and Price, 1997; Virtanen et al., 2020). We chose Differential Evolution due to its gradient free nature and ability to overcome local minima (Storn and Price, 1997). After an initial Sobol' sequence sampling (Sobol', 1967), the algorithm draws parameter candidate samples from the parameter space by mutating the current best member of the sample population with the difference of two other randomly chosen members. After the global optimization with the Differential Evolution algorithm, the result is refined by the L-BFGS-B method of Byrd et al. (1995) which is a Quasi-Newtonian method that estimates the Hessian of the objective function based on the recent parameter sample history and can handle bound constraints.

https://doi.org/10.5194/gmd-2022-258
Preprint. Discussion started: 16 January 2023


Geoscientific Model Development Discussions

We optimize the model by minimizing the root mean squared error (RMSE) which is a measure of the distance between the predicted values from the model $\hat{\boldsymbol{y}}$ to the reference $\boldsymbol{y}$. It is defined as

$$\mathrm{RMSE}(y,\hat{y}) = \sqrt{\frac{1}{n}\sum_{i=1}^{n}(\hat{y}_i - y_i)^2} \tag{6}$$

with y_i and $\hat{y}_i$ being the i-th element of the $i = 1, ..., n$ elements in $\boldsymbol{y}$ and $\hat{\boldsymbol{y}}$, respectively. Additionally, we use the two statistical error measures coefficient of determination (R^2) and BIAS in order to evaluate the model. The R^2 score is representing the proportion of variation in the data y that can be predicted from the model and is defined as

$$R^2(y,\hat{y}) = 1 - \frac{\sum_{i=1}^{n}(y_i - \hat{y}_i)^2}{\sum_{i=1}^{n}(y_i - \bar{y})^2} \tag{7}$$

with $\hat{y}_i$ being the predicted value of the i-th sample, y_i being the associated reference value for total n samples and $\bar{y}$ being the mean of $\boldsymbol{y}$. The BIAS is a measure for the systematic tendency of a model to over- or under represent the reference data. Therefore, it has large implications in climatological contexts. We calculate the BIAS for a sample of size n as follows:

$$\mathrm{BIAS}(y,\hat{y}) = \frac{1}{n}\sum_{i=1}^{n} y_i - \hat{y}_i \tag{8}$$

where $\hat{y}_i$ is the predicted value of the i-th sample and y_i is the associated reference value. All presented score values RMSE, R^2 and BIAS are calculated only for the subset of $\hat{\boldsymbol{y}}$ and $\boldsymbol{y}$ where any of the two vectors is not zero.

In order to assess the importance of individual model parameters on the result, we perform a sensitivity analysis on the validation data set by calculating R^2 and BIAS on 114688 parameter sets sampled after the method of Saltelli (2002) and calculate the global sensitivity indices (S_{Ti}) after Sobol' (2001). These indices give an estimate about the proportion of variance in R^2 and BIAS that can be attributed to a model parameter and all its interactions with other model parameters. We perform the sensitivity analysis within the Python framework *SALib* of Herman and Usher (2017).

3.1 Data from Swiss manual observer stations

For calibrating the SWE2HS model, we use data from 58 Swiss manual observer stations between 1080 and 2620 m a.s.l. operated by the WSL Institute for Snow and Avalanche Research SLF (Marty et al., 2017). Snow depth is measured daily with a snow stake and SWE is measured every two weeks in a snow pit on the same site. In order to get daily SWE data, HS data is transformed to SWE with the ΔSNOW model of Winkler et al. (2021). In order to improve the accuracy of the daily SWE time series, the ΔSNOW model parameters were optimized for each station individually using the biweekly SWE measurements from the manual observer profiles. Due to its destructive nature, the snow pit is not at the exact same location as the snow stake and consequently the profile cut height can deviate from the measured height at the snow stake. Therefore, the biweekly SWE data were corrected by calculating the bulk density from the profile and applying it to the measured height from the snow stake. ΔSNOW model parameter optimization was done by minimizing the RMSE between modeled SWE and corrected SWE from the profiles while we allowed the ΔSNOW parameters ρ_{max} (maximum density) to vary between 300 and 600 $\mathrm{kg\,m^{-3}}$, ρ_0

https://doi.org/10.5194/gmd-2022-258
Preprint. Discussion started: 16 January 2023

Geoscientific Model Development Discussions
Open Access
EGU

Table 1. Automatic weather stations from which we used snow water equivalent and snow depth data for validation of the model. The number of years refers to complete hydrological years (Sep-Aug) included after data cleaning, the average snow depth ($\overline{\text{HS}}$) is calculated in the winter months from November to April.

Site name	Source	Altitude [m a.s.l.]	#years of data	$\overline{\text{HS}}$ (Nov-Apr) [m]
Col de Porte (FR)	Lejeune et al. (2019)	1325	13	0.51
Davos (CH)	SLF	1563	1	0.48
Fellhorn (DE)	LWZ Bavaria	1610	14	0.88
Kühroint (DE)	LWZ Bavaria	1420	13	0.75
Kühtai (AT)	Krajci et al. (2017)	1920	21	0.80
Laret (CH)	SLF	1513	2	0.69
Spitzingsee (DE)	LWZ Bavaria	1100	9	0.47
Wattener Lizum (AT)	BFW Innsbruck	1994	8	0.59
Weissfluhjoch (CH)	SLF	2536	12	1.35
Zugspitze (DE)	LWZ Bavaria	2420	9	1.64

(new snow density) to vary between 65 and 135 $\mathrm{kg\,m^{-3}}$, and the remaining parameters to vary by $\pm 25\,\%$ from the optimized value found in Winkler et al. (2021). For optimization, we again used Differential Evolution as described in Sect 3. In order to further increase the reliability of the calibration data set, we only kept station-winters with more than 2 SWE profiles and RMSE below 7.5 mm in the resulting daily SWE data set from the ΔSNOW model. Since we did not want certain stations with long SWE and HS records to bias the calibration, we shortened the length of station records longer than 15 years by randomly selecting 15 water years from the full station record. The resulting set consists of 741 station-years from 58 stations. Compared with the biweekly manual SWE measurements, the modeled daily SWE calibration set has an RMSE of 30.0 mm and BIAS of -1.09 mm. We however cannot assess the uncertainty for the dates between the biweekly SWE measurements.

While we are aware that it might be preferable to calibrate a model on measured data instead of output from another model, we still chose the above described approach in order to have an exhaustive calibration data set which a) covers a wider range of altitudes, expositions and snow climatic settings in our target region, b) does not have problems of potential over- and under measurement from automatic SWE measurement devices (Johnson and Marks, 2004), and c) does not contain measurement noise which is not properly tackled in the SWE2HS model.

3.2 Data from automatic weather stations in the European Alps

As validation data set, we gathered data of 10 different automatic weather stations (AWSs) in Austria, France, Germany, and Switzerland that automatically measure SWE with either a snow pillow or a snow scale and measure snow depth with an ultrasonic measurement device at sub-daily resolution (see Table 1). The raw SWE and HS data with a temporal resolution ranging between 15 min and 1 h were resampled to daily resolution by taking the median of all measurements between 6 a.m. and

https://doi.org/10.5194/gmd-2022-258
Preprint. Discussion started: 16 January 2023

Geoscientific Model Development Discussions
Open Access
EGU

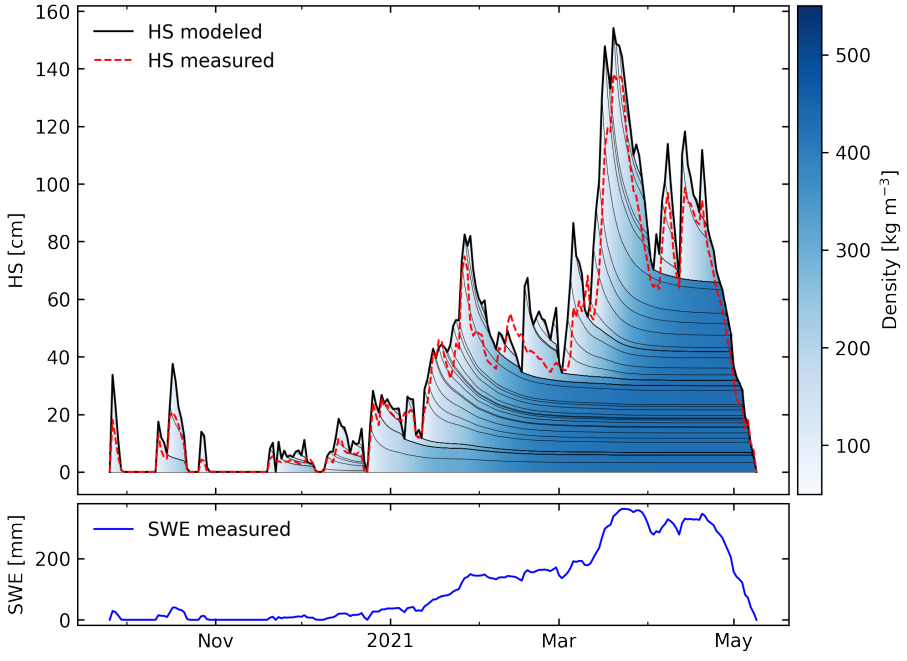

Figure 1. Schematic modeled snow pack evolution for the station Kühroint (validation data set, see Table 1) in the winter 2020/21. The red dotted line is the measured snow depth (HS), the black solid line bounding the colored area is the modeled snow depth, the thin black lines depict the layer borders within the modeled snowpack, and the coloring refers to the modeled layer densities. The bottom panel shows the daily snow water equivalent time series which was used to force the model.

8 a.m. local time. Any systematic offset errors from raw sensors were corrected by subtracting the mode of the summer months (MJJASON) from the SWE or HS time series of each hydrological year. Missing data gaps shorter than 5 consecutive days in SWE have been filled by linear interpolation. For longer gaps, the time period before the gap in the respective hydrological year is included and data after the gap is discarded. Short gaps in snow depth are accepted since it is not required to drive the density model but for evaluating the quality of the model. Missing HS data points will thus not be included when calculating any score metrics. All hydrological years that were included in the final validation data set have been quality checked by visual inspection and by ensuring the bulk density stays below 700 $\mathrm{kg\,m^{-3}}$.

4 Results

The model calibration on the data set described in Sect. 3.1 yielded the optimized parameters listed in Table 2. Figure 1 shows the temporal evolution during an example winter at the station Kühroint (AWS station, see Table 1) calculated with the optimized parameter set. Looking at the temporal development of the density and layering in the modeled snow pack, the density rapidly increases in the first few days after layer creation leading to enhanced settlement in this period. Additionally, the density of a layer reacts to changes in SWE in the overlying layers (see e.g. bottom three layers, end of January 2021).

https://doi.org/10.5194/gmd-2022-258
Preprint. Discussion started: 16 January 2023

Geoscientific Model Development Discussions
Open Access
EGU

Table 2. Parameters of the model, lower and upper bounds during calibration and optimized value.

Parameter	Description	Unit	Lower bound	Upper bound	Optimized value
$\rho_{max,init}$	Initial maximum density	$\mathrm{kg\,m^{-3}}$	150.00	300.00	204.135
$\rho_{max,end}$	Final maximum density	$\mathrm{kg\,m^{-3}}$	300.00	600.00	427.181
ρ_{new}	New snow density	$\mathrm{kg\,m^{-3}}$	50.00	150.00	85.914
R	Settling resistance	-	1.00	110.00	5.923
σ_{max}	Overburden where $\rho_{max,end}$ is reached	mmw.e.	100	2000	227
v_{melt}	Speed of melt metamorphism transition	-	0.05	2.00	0.134

Table 3. Scores values RMSE, R^2 and BIAS for the calibration and validation data set after parameter calibration. The accompanying data is visualized in Figs. 2 and 3.

	RMSE [cm]	R^2	BIAS [cm]
Manual observer stations	8.4	0.971	-0.3
Automatic snow stations	20.5	0.919	2.5

With the optimized parameter set, the model is able to fit the calibration data with RMSE of 8.4 cm, R^2 of 0.97 and negligible BIAS of 0.2 cm (see Table 3 and Fig. 2, left panel). The seasonal evolution of the bulk density can be reproduced well on the calibration data set with June being the only month with considerable underestimation of the median snow depth (Fig. 3, left panel). On the validation data set, the performance is weaker than for the calibration data set with RMSE of 20.5 cm, R^2 of 0.92 and BIAS of 2.5 cm. The model slightly underestimates the median snow depth in February and March on the validation data set and overestimates the median snow depth in the ablation months April, May and June. On the calibration data set, R^2 is for 75% of the stations above 0.95, only for two stations R^2 is below 0.8 (see Fig. 4). On the validation data set, R^2 per station varies between 0.15 and 0.95 and is larger than 0.75 for 75% of the stations. On the calibration data set, the BIAS per station is uniformly distributed around 0 and for all except of two stations smaller than ± 10 cm. On the validation data set, the BIAS per station is ranging from -7 cm to 22.7 cm with four stations having a positive BIAS larger tan 10 cm.

According to the sensitivity analysis, the settling resistance factor R is the most important model parameter with a global sensitivity index of 0.44 and 0.43 for R^2 and BIAS respectively (Fig. 5). This means, that within the 114688 samples drawn during the sensitivity analysis, 44% and 43% of the proportion of variance in in R^2 and BIAS can be attributed to the settling resistance factor R, respectively (see Sect. 3). For R^2, the second most influential model parameter is new snow density ρ_{new} followed by the final maximum snow density $\rho_{max,end}$. For BIAS, the model is less sensitive to ρ_{new} than for R^2. The model is relatively insensitive to changes in the model parameters $rho_{max,init}$, v_{melt}, and σ_{max} with total sensitivity indices below 0.1 for both R^2 and RMSE.

https://doi.org/10.5194/gmd-2022-258
Preprint. Discussion started: 16 January 2023

Geoscientific Model Development Discussions

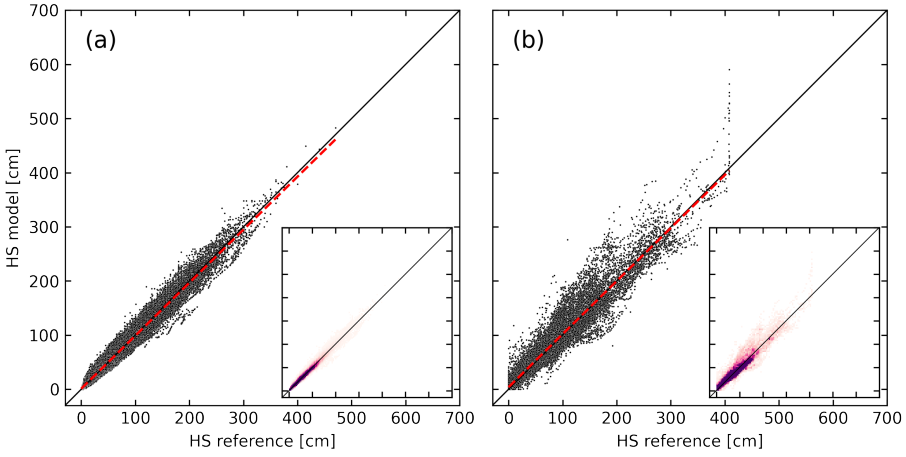

Figure 2. Scatterplots of modeled against measured snow depth values for (a) the calibration data set from Swiss manual observer stations and (b) the validation data set from automatic snow stations. The red dashed line is a linear fit to the data, the black solid line represents perfect predictions. In the insets, the same data is shown as bivariate histograms indicating the density of the scatter points. Score values of the shown data are listed in Table 3.

5 Discussion

5.1 Model complexity selection

On our way towards the model presented here, we tried models of different complexity, included and removed processes while iterating back and forward. Some prototype model versions additionally included daily temperature as input forcing, which we tried to use for parametrization of new snow density and onset of the wetting from top of the snowpack by using the cold content parameterizations used in Scheppler (2000) and Szentimrey et al. (2012). Other versions parametrized the settling resistance R based on overburden or density of a layer or a combination of the two factors. In order to do an objective model selection for a final model version, additionally to the scores defined in Sect. 3 we calculated the Akaike Information Criterion (AIC) by using the RMSE as an estimator for the maximum value of the likelihood function. The AIC is a statistical error measure that penalizes larger numbers of free model parameters. We then ranked the 4 different scores for the optimized model of each version and averaged the score ranks over the calibration and validation data set. This allowed us to make an informed decision on which model version to use. In order to avoid overfitting on the calibration data set, we gave more focus on the validation data set.

We assumed it would be beneficial to use temperature in the beginning of model conceptualization and one could argue, that when using SWE from an accumulation and ablation model, there is always at least daily mean temperature available used to drive a melt model. However, when quantitatively assessing the model versions with parametrized new snow density or cold content parameterizations we did not see model improvement from the daily mean temperature inclusion and thus decided to only use SWE. This additionally comes with the asset that the model can be plugged in as a post-processing tool to

https://doi.org/10.5194/gmd-2022-258
Preprint. Discussion started: 16 January 2023

Geoscientific Model Development Discussions
Open Access
EGU

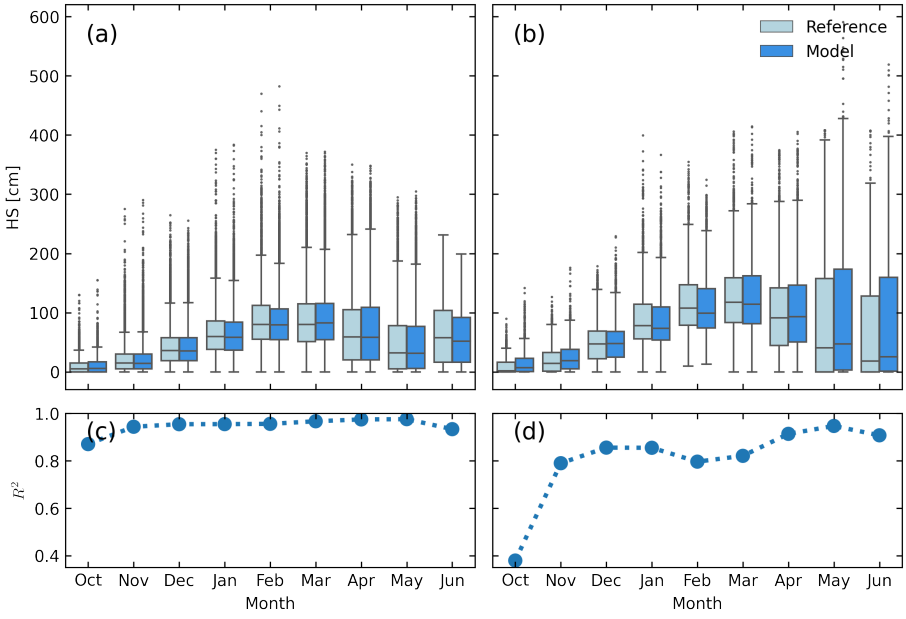

Figure 3. Boxplots comparing the distributions of measured and modeled data in the months from October to June for (a) the calibration data set from Swiss manual observer stations and (b) the validation data set from automatic snow stations. A box spans the lower and upper quartile of the data with a line at the median. The whiskers extend to last datum within 1.5 times the interquartile range while the points represent outliers past the range of the whiskers. The lower two panels show R^2 scores for the modeled data to the reference calculated for the calibration data set (c) and the validation data set (d).

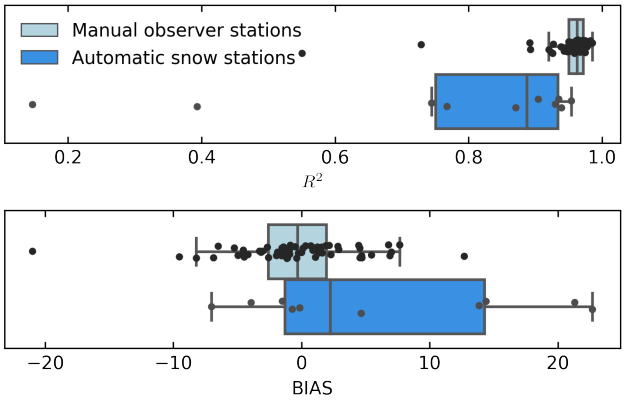

Figure 4. Boxplots of the scores R^2, and BIAS calculated individually on the data from each station in the calibration data set (light blue) and validation data set (dark blue). The black dots show the underlying data from which the boxplots were calculated.

any snow model which outputs daily SWE. Besides the best performance, another important factor to keep the model simple

https://doi.org/10.5194/gmd-2022-258
Preprint. Discussion started: 16 January 2023

Geoscientific Model Development Discussions

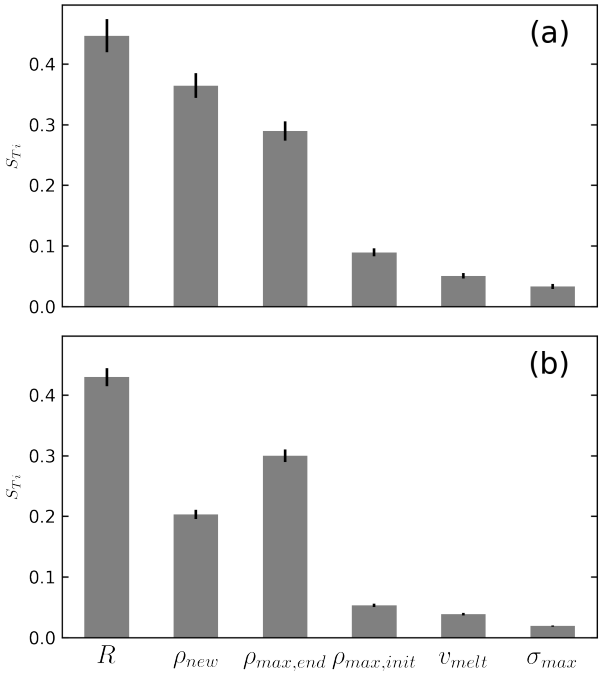

Figure 5. Global Sobol' (2001) sensitivity indices (S_{Ti}) calculated for (a) R^2 and (b) BIAS of the model predictions on the AWS data set from 114688 samples drawn with the method of Saltelli (2002).

was to reduce the risk of equifinality, meaning that an optimal solution can be achieved through different states i.e. parameter combinations of the model (Beven and Freer, 2001).

5.2 General remarks and limitations

As shown in Sect. 4, the model is able to fit the calibration data very well. The calibration data has been compiled from manually measured snow depth data and modeled SWE data with the ΔSNOW model of Winkler et al. (2021). Therefore, e.g. the occurrence of rain-on-snow events cannot degrade the model skill since the ΔSNOW model is also not able to represent rain-on-snow events. We still consider using modeled data for calibration a valid approach as we hold back a set of measured data for independent validation of our optimized model parameter set (see Sect. 3.2). Additionally, SWE2HS' main scope of application is post-processing output from simple accumulation and melt models. The model is performing better on the ΔSNOW data set compared to the AWSs data set. This is due to several reasons. First and foremost, the model has been calibrated on the data in the ΔSNOW data set and not on the data in the AWSs data set. Accordingly, the fitted parameters do not necessarily suite the data in the AWSs data set. Other reason for weaker model performance in the AWSs data set are potentially arising from noise and measurement uncertainties. One source of these uncertainties are problems of over- and under measurement from the automatic SWE measurement devices (Johnson and Marks, 2004). This uncertainty increases with time during the winter

https://doi.org/10.5194/gmd-2022-258
Preprint. Discussion started: 16 January 2023

Geoscientific Model Development Discussions

and could be an explanation for the overestimation in the ablation season. Additionally, the measurement uncertainty of the automatic SWE and HS data can cause small changes in SWE and HS, which are not physically based (Capelli et al., 2022). In this regard the SWE and HS in the calibration data set is much more consistent. We could not include a mechanism to deal with measurement uncertainties analogous to Winkler et al. (2021) since a SWE time series does not contain any information on settlement which could be used to correctly distinguish a signal from noise. A last source of uncertainty in the AWSs data set is that the automatic SWE measurements are not necessarily located at the exact same place as the snow depth measurements and we did not have a way to correct this error in the same way as we did for the manually observed SWE and HS measurements.

Other sources of uncertainty are due to inherent limitations of our semi-empirical modeling approach. As mentioned above, the model is not able to represent rain-on-snow events. In the exemplary snow pack evolution of the winter 2020/21 at station Kühroint, an increase in SWE causes modeled snow depth to increase although the measured snow depth is constantly decreasing during this time (mid of March 2021, Fig. 1). This could be an example of either erroneously measured SWE or a rain-on-snow event which caused an increase in SWE but not in HS. The latter seems more likely since simultaneously to the increase in SWE, settling is enhanced for the measured HS and (as additional not-shown data demonstrates) the temperature is rising above $0\,^{\circ}\mathrm{C}$ in combination with precipitation. Morán-Tejeda et al. (2016) show that such events are rare and contribute to maximum $100\,\mathrm{mm}$ for elevations above $2000\,\mathrm{m\,a.s.l.}$ With a changing climate, rain-on-snow events might become more likely above $2000\,\mathrm{m\,a.s.l.}$ but might decrease for low altitudes as a decrease in rainfall and shorter snow cover duration are thought to counteract increased temperatures. Another limitation of the model is the inability to properly track the wetting front which is propagating top to bottom through the snowpack over time (Marsh and Woo, 1984). Due to the choice of only using SWE as forcing, we can only detect the wetting front reaching the bottom which will be observable as a negative change in SWE. Therefore, the model will likely miss the onset of the melt metamorphism in the snow pack for the upper layers. We try to partly compensate for this flaw by increasing the maximum density with increasing overburden. As R^2 is not decreasing in spring (Fig. 3) for the calibration and validation data set, the model seems to be able to predict snow depth during the ablation period reasonably well nevertheless. Since the model is of empirical nature, the parameter set which is presented here for the European Alps might not be suited for other regions on earth with different climatologic conditions. If applied to other regions, the model parameters need to be calibrated again. However, as we never tested the model in e.g. Arctic regions, we cannot make any statements if the model is able to represent settling dynamics in these snow climatologic conditions even if it would be calibrated on data from there. Although the calibrated parameter set presented in this paper is thought to be representative for the European Alps, it can be quite off for some stations in the validation data set with BIAS of up to $22.7\,\mathrm{cm}$ (see Fig. 4). This high positive BIAS is occurring at station Davos (only one year of data) and station Laret (two years of data). We suspect that in all three years a short period of potential positive measurement errors from the SWE sensor caused the snow cover evolution to become defective. In order to achieve the best model skill for a single location, recalibrating the model to data from that location is necessary.

Simple empirical models that try to conceptualize processes in a non-physical way are often subject to the risk of potential model equifinality (Beven and Freer, 2001). While we chose to present a single calibrated parameter set in Sect. 4, there is still

https://doi.org/10.5194/gmd-2022-258
Preprint. Discussion started: 16 January 2023


Geoscientific Model Development Discussions

the risk that other parameter sets might lead to equally good predictions. However, an in-depth analysis of potential equifinality is out of scope of this model description paper and might be subject of future work.

The model is less sensitive to changes in the model parameter ρ_{new} (new snow density) for BIAS than for R^2. This is likely due to the nature of the two statistical error metrics used. R^2 is measuring the proportion of variance the model is able to explain in the data and the BIAS is measuring if the model is on average under or overestimating the data to be predicted. The new snow density is mainly affecting the model result for the times shortly following increases of SWE and thus is not as important for model BIAS as for R^2. Due to the sensitivity to new snow density and the fixed new snow density approach in the model it is not reasonable to derive climatologic indices related to the amount of new snow such as the maximum increase in HS during three days from model output.

6 Conclusions

We present a simple snow density model which can be used to transfer continuous daily snow water equivalent data to snow depth. The semi-empirical multi-layer model uses exponential settling equations, a fixed new snow density and assumes a changing maximum snow density over time based on overburden and SWE losses. The model is validated on multi-year data from 10 automatic snow stations between 1100 and 2500 $\mathrm{m\,a.s.l.}$ in the European Alps where it can reproduce the measured data with RMSE of 20.5 cm and BIAS of 2.5 cm. Due to its simplicity, the model can be used for climatological use cases where input data for more sophisticated densification models is sparse. Since the only input needed to drive the model is daily SWE, it can be also used to post-process model output from any other snow model or to transfer SWE data obtained from automatic SWE sensors.

Code availability. The current version of the model source code, including documentation and examples is available at https://code.wsl.ch/aschauer/swe2hs (last access: 20.10.2022) and a Python package is available through PyPI at https://pypi.org/project/swe2hs/ (last access: 20.10.2022). The exact version that was used for this manuscript (v1.0.3) is archived at https://doi.org/10.5281/zenodo.7228066 (Aschauer, 2022).

Data availability. The data from Kühtai is described in Krajci et al. (2017) and is available from https://doi.org/10.5281/zenodo.556110. The data from Col de Porte is described in Lejeune et al. (2019) and is avaliable from https://doi.org/10.17178/CRYOBSCLIM.CDP.2018. The complete validation data set is available from the authors upon request. The data set used for calibration will be made publicly available by the time of publication of the manuscript.

https://doi.org/10.5194/gmd-2022-258
Preprint. Discussion started: 16 January 2023


Geoscientific Model Development Discussions

Author contributions. JA compiled the calibration and validation sets, developed the methodology and software code, and wrote the initial paper draft. CM, TJ and AM gave input to the methodology and reviewed different model versions. CM acquired funding and supervised the study. All authors reviewed and commented on the manuscript.

Competing interests. The authors declare that they have no competing interests.

Acknowledgements. We want to thank the Bavarian avalanche warning center (Lawinenwarnzentrale Bayern) in Munich and the Austrian Research Centre for Forests BFW in Innsbruck for contributing data from their measurement stations to the calibration data set. This work was financially supported by the internal project "Climatological maps for snow depth" of the Swiss Federal Institute for Forest Snow and Landscape Research WSL.

https://doi.org/10.5194/gmd-2022-258
Preprint. Discussion started: 16 January 2023

Geoscientific Model Development Discussions

References

Aili, T., Soncini, A., Bianchi, A., Diolaiuti, G., D'Agata, C., and Bocchiola, D.: Assessing water resources under climate change in high-altitude catchments: a methodology and an application in the Italian Alps, Theoretical and Applied Climatology, 135, 135–156, https://doi.org/10.1007/s00704-017-2366-4, 2019.

Anderson, E. A.: A point energy and mass balance model of a snow cover, NOAA Technical Report NWS 19, Office of Hydrology, National Weather Service, Silver Spring, Maryland, 1976.

Aschauer, J.: swe2hs Python package, https://doi.org/10.5281/zenodo.7228066, 2022.

Bartelt, P. and Lehning, M.: A physical SNOWPACK model for the Swiss avalanche warning: Part I: numerical model, Cold Regions Science and Technology, 35, 123–145, https://doi.org/10.1016/S0165-232X(02)00074-5, 2002.

Beven, K. and Freer, J.: Equifinality, data assimilation, and uncertainty estimation in mechanistic modelling of complex environmental systems using the GLUE methodology, Journal of hydrology, 249, 11–29, 2001.

Brown, R., Bartlett, P., MacKay, M., and Verseghy, D.: Evaluation of snow cover in CLASS for SnowMIP, Atmosphere-Ocean, 44, 223–238, https://doi.org/10.3137/ao.440302, 2006.

Brown, R. D., Brasnett, B., and Robinson, D.: Gridded North American monthly snow depth and snow water equivalent for GCM evaluation, Atmosphere-Ocean, 41, 1–14, https://doi.org/10.3137/ao.410101, 2003.

Brun, E., David, P., Sudul, M., and Brunot, G.: A numerical model to simulate snow-cover stratigraphy for operational avalanche forecasting, Journal of Glaciology, 38, 13–22, https://doi.org/10.3189/S0022143000009552, 1992.

Byrd, R. H., Lu, P., Nocedal, J., and Zhu, C.: A Limited Memory Algorithm for Bound Constrained Optimization, SIAM Journal on Scientific Computing, 16, 1190–1208, https://doi.org/10.1137/0916069, 1995.

Capelli, A., Koch, F., Henkel, P., Lamm, M., Appel, F., Marty, C., and Schweizer, J.: GNSS signal-based snow water equivalent determination for different snowpack conditions along a steep elevation gradient, The Cryosphere, 16, 505–531, https://doi.org/10.5194/tc-16-505-2022, 2022.

Dask Development Team: Dask: Library for dynamic task scheduling, https://dask.org, 2016.

Dawson, N., Broxton, P., and Zeng, X.: A new snow density parameterization for land data initialization, Journal of Hydrometeorology, 18, 197–207, https://doi.org/10.1175/jhm-d-16-0166.1, 2017.

Essery, R.: A factorial snowpack model (FSM 1.0), Geoscientific Model Development, 8, 3867–3876, https://doi.org/10.5194/gmd-8-3867-2015, 2015.

Gugerli, R., Salzmann, N., Huss, M., and Desilets, D.: Continuous and autonomous snow water equivalent measurements by a cosmic ray sensor on an alpine glacier, The Cryosphere, 13, 3413–3434, https://doi.org/10.5194/tc-13-3413-2019, 2019.

Guyennon, N., Valt, M., Salerno, F., Petrangeli, A. B., and Romano, E.: Estimating the snow water equivalent from snow depth measurements in the Italian Alps, Cold Regions Science and Technology, 167, 102 859, 2019.

Hanzer, F., Helfricht, K., Marke, T., and Strasser, U.: Multilevel spatiotemporal validation of snow/ice mass balance and runoff modeling in glacierized catchments, The Cryosphere, 10, 1859–1881, https://doi.org/10.5194/tc-10-1859-2016, 2016.

Harris, C. R., Millman, K. J., Van Der Walt, S. J., Gommers, R., Virtanen, P., Cournapeau, D., Wieser, E., Taylor, J., Berg, S., Smith, N. J., et al.: Array programming with NumPy, Nature, 585, 357–362, 2020.

Helfricht, K., Hartl, L., Koch, R., Marty, C., and Olefs, M.: Obtaining sub-daily new snow density from automated measurements in high mountain regions, Hydrology and Earth System Sciences, 22, 2655–2668, https://doi.org/10.5194/hess-22-2655-2018, 2018.

https://doi.org/10.5194/gmd-2022-258
Preprint. Discussion started: 16 January 2023

Herman, J. and Usher, W.: SALib: An open-source Python library for Sensitivity Analysis, The Journal of Open Source Software, 2, https://doi.org/10.21105/joss.00097, 2017.

Hoyer, S. and Hamman, J.: xarray: N-D labeled arrays and datasets in Python, Journal of Open Research Software, 5, https://doi.org/10.5334/jors.148, 2017.

Johnson, J. B. and Marks, D.: The detection and correction of snow water equivalent pressure sensor errors, Hydrological Processes, 18, 3513–3525, https://doi.org/10.1002/hyp.5795, 2004.

Jonas, T., Marty, C., and Magnusson, J.: Estimating the snow water equivalent from snow depth measurements in the Swiss Alps, Journal of Hydrology, 378, 161–167, https://doi.org/10.1016/j.jhydrol.2009.09.021, 2009.

Jordan, R.: A one-dimensional temperature model for a snow cover: Technical documentation for SNTHERM. 89, Special Report 91-16, U.S. Army Corps of Engineers, Cold Regions Research and Engineering Laboratory, 1991.

Kinar, N. J. and Pomeroy, J. W.: Measurement of the physical properties of the snowpack, Reviews of Geophysics, 53, 481–544, https://doi.org/10.1002/2015RG000481, 2015.

Koch, F., Henkel, P., Appel, F., Schmid, L., Bach, H., Lamm, M., Prasch, M., Schweizer, J., and Mauser, W.: Retrieval of Snow Water Equivalent, Liquid Water Content, and Snow Height of Dry and Wet Snow by Combining GPS Signal Attenuation and Time Delay, Water Resources Research, 55, 4465–4487, https://doi.org/https://doi.org/10.1029/2018WR024431, 2019.

Krajci, P., Kirnbauer, R., Parajka, J., Schöber, J., and Blöschl, G.: The Kühtai data set: 25 years of lysimetric, snow pillow, and meteorological measurements, Water Resources Research, 53, 5158–5165, https://doi.org/10.1002/2017WR020445, 2017.

Lam, S. K., Pitrou, A., and Seibert, S.: Numba: A LLVM-Based Python JIT Compiler, in: Proceedings of the Second Workshop on the LLVM Compiler Infrastructure in HPC, LLVM '15, Association for Computing Machinery, New York, NY, USA, https://doi.org/10.1145/2833157.2833162, 2015.

Lawrence, D. M., Fisher, R. A., Koven, C. D., Oleson, K. W., Swenson, S. C., Bonan, G., Collier, N., Ghimire, B., van Kampenhout, L., Kennedy, D., Kluzek, E., Lawrence, P. J., Li, F., Li, H., Lombardozzi, D., Riley, W. J., Sacks, W. J., Shi, M., Vertenstein, M., Wieder, W. R., Xu, C., Ali, A. A., Badger, A. M., Bisht, G., van den Broeke, M., Brunke, M. A., Burns, S. P., Buzan, J., Clark, M., Craig, A., Dahlin, K., Drewniak, B., Fisher, J. B., Flanner, M., Fox, A. M., Gentine, P., Hoffman, F., Keppel-Aleks, G., Knox, R., Kumar, S., Lenaerts, J., Leung, L. R., Lipscomb, W. H., Lu, Y., Pandey, A., Pelletier, J. D., Perket, J., Randerson, J. T., Ricciuto, D. M., Sanderson, B. M., Slater, A., Subin, Z. M., Tang, J., Thomas, R. Q., Val Martin, M., and Zeng, X.: The Community Land Model Version 5: Description of New Features, Benchmarking, and Impact of Forcing Uncertainty, Journal of Advances in Modeling Earth Systems, 11, 4245–4287, https://doi.org/10.1029/2018MS001583, 2019.

Lehning, M., Bartelt, P., Brown, B., Fierz, C., and Satyawali, P.: A physical SNOWPACK model for the Swiss avalanche warning: Part II. Snow microstructure, Cold Regions Science and Technology, 35, 147–167, https://doi.org/10.1016/S0165-232X(02)00073-3, 2002.

Lejeune, Y., Dumont, M., Panel, J.-M., Lafaysse, M., Lapalus, P., Le Gac, E., Lesaffre, B., and Morin, S.: 57 years (1960–2017) of snow and meteorological observations from a mid-altitude mountain site (Col de Porte, France, 1325 m of altitude), Earth System Science Data, 11, 71–88, https://doi.org/10.5194/essd-11-71-2019, 2019.

Marke, T., Strasser, U., Hanzer, F., Stötter, J., Wilcke, R. A. I., and Gobiet, A.: Scenarios of future snow conditions in Styria (Austrian Alps), Journal of Hydrometeorology, 16, 261–277, https://doi.org/10.1175/jhm-d-14-0035.1, 2015.

Marke, T., Hanzer, F., Olefs, M., and Strasser, U.: Simulation of past changes in the Austrian snow cover 1948–2009, Journal of Hydrometeorology, 19, 1529–1545, https://doi.org/10.1175/jhm-d-17-0245.1, 2018.

https://doi.org/10.5194/gmd-2022-258
Preprint. Discussion started: 16 January 2023

Marsh, P. and Woo, M.-K.: Wetting front advance and freezing of meltwater within a snow cover: 1. Observations in the Canadian Arctic, Water Resources Research, 20, 1853–1864, https://doi.org/10.1029/WR020i012p01853, 1984.

Martinec, J.: Zimni prognosy s pouzitim radioisotopu (Winter forecasts with the use of radioisotopes), Vltavska kaskada (The Vltava reservoir system), VUV Praha-Podbab, Praha, Czech Republic, pp. 45–60, 1956.

Martinec, J.: Expected Snow Loads on Structures from Incomplete Hydrological Data, Journal of Glaciology, 19, 185–195, https://doi.org/10.3189/S0022143000029270, 1977.

Marty, C., Tilg, A.-M., and Jonas, T.: Recent evidence of large-scale receding snow water equivalents in the European Alps, Journal of Hydrometeorology, 18, 1021–1031, 2017.

McCreight, J. L. and Small, E. E.: Modeling bulk density and snow water equivalent using daily snow depth observations, The Cryosphere, 8, 521–536, 2014.

Meister, R.: Density of new snow and its dependence on air temperature and wind, in: Workshop on the Correction of Precipitation Measurements, Zurich 1–3 April, pp. 73–79, 1986.

Mizukami, N. and Perica, S.: Spatiotemporal characteristics of snowpack density in the mountainous regions of the western United States, Journal of Hydrometeorology, 9, 1416–1426, 2008.

Morán-Tejeda, E., López-Moreno, J. I., Stoffel, M., and Beniston, M.: Rain-on-snow events in Switzerland: recent observations and projections for the 21st century, Climate Research, 71, 111–125, https://www.jstor.org/stable/24897493, 2016.

Olefs, M., Koch, R., Schöner, W., and Marke, T.: Changes in Snow Depth, Snow Cover Duration, and Potential Snowmaking Conditions in Austria, 1961–2020—A Model Based Approach, Atmosphere, 11, 1330, https://doi.org/10.3390/atmos11121330, 2020.

Pistocchi, A.: Simple estimation of snow density in an Alpine region, Journal of Hydrology: Regional Studies, 6, 82–89, 2016.

Reback, J., jbrockmendel, McKinney, W., den Bossche, J. V., Augspurger, T., Roeschke, M., Hawkins, S., Cloud, P., gfyoung, Sinhrks, Hoefler, P., Klein, A., Petersen, T., Tratner, J., She, C., Ayd, W., Naveh, S., Darbyshire, J., Garcia, M., Shadrach, R., Schendel, J., Hayden, A., Saxton, D., Gorelli, M. E., Li, F., Zeitlin, M., Jancauskas, V., McMaster, A., Wörtwein, T., and Battiston, P.: pandas-dev/pandas: Pandas, https://doi.org/10.5281/zenodo.3509134, 2022.

Saltelli, A.: Making best use of model evaluations to compute sensitivity indices, Computer Physics Communications, 145, 280–297, https://doi.org/10.1016/S0010-4655(02)00280-1, 2002.

Scheppler, P.: Schneedeckenmodellierung und Kalibrierungsmöglichkeiten für ausgewählte Beobachtungsstationen, PhD Thesis, Diplomarbeit Universität Bern, Schweiz, 2000.

Sobol', I. M.: On the distribution of points in a cube and the approximate evaluation of integrals, Zhurnal Vychislitel'noi Matematiki i Matematicheskoi Fiziki, 7, 784–802, 1967.

Sobol', I. M.: Global sensitivity indices for nonlinear mathematical models and their Monte Carlo estimates, Mathematics and Computers in Simulation, 55, 271–280, https://doi.org/10.1016/S0378-4754(00)00270-6, 2001.

Sommerfeld, R. A. and LaChapelle, E.: The Classification of Snow Metamorphism, Journal of Glaciology, 9, 3–18, https://doi.org/10.3189/S0022143000026757, 1970.

Storn, R. and Price, K.: Differential Evolution – A Simple and Efficient Heuristic for global Optimization over Continuous Spaces, Journal of Global Optimization, 11, 341–359, https://doi.org/10.1023/A:1008202821328, 1997.

Szentimrey, T., Lakatos, M., Bihari, Z., Kovács, T., Németh, A., Szalai, S., Auer, I., Hiebl, J., Milkovic, J., and Zahradnicek, P.: Final report on the creation of national gridded datasets, per country, Carpatclim project deliverable d 2.9, Hungarian Meteorological Service, 2012.

https://doi.org/10.5194/gmd-2022-258
Preprint. Discussion started: 16 January 2023

Valt, M., Guyennon, N., Salerno, F., Petrangeli, A. B., Salvatori, R., Cianfarra, P., and Romano, E.: Predicting new snow density in the Italian Alps: A variability analysis based on 10 years of measurements, Hydrological Processes, 32, 3174–3187, https://doi.org/10.1002/hyp.13249, 2018.

van Kampenhout, L., Lenaerts, J. T. M., Lipscomb, W. H., Sacks, W. J., Lawrence, D. M., Slater, A. G., and van den Broeke, M. R.: Improving the Representation of Polar Snow and Firn in the Community Earth System Model, Journal of Advances in Modeling Earth Systems, 9, 2583–2600, https://doi.org/10.1002/2017MS000988, 2017.

Vionnet, V., Brun, E., Morin, S., Boone, A., Faroux, S., Moigne, P. L., Martin, E., and Willemet, J.-M.: The detailed snowpack scheme Crocus and its implementation in SURFEX v7.2, Geoscientific Model Development, 5, 773–791, https://doi.org/10.5194/gmd-5-773-2012, 2012.

Virtanen, P., Gommers, R., Oliphant, T. E., Haberland, M., Reddy, T., Cournapeau, D., Burovski, E., Peterson, P., Weckesser, W., Bright, J., van der Walt, S. J., Brett, M., Wilson, J., Millman, K. J., Mayorov, N., Nelson, A. R. J., Jones, E., Kern, R., Larson, E., Carey, C. J., Polat, I., Feng, Y., Moore, E. W., VanderPlas, J., Laxalde, D., Perktold, J., Cimrman, R., Henriksen, I., Quintero, E. A., Harris, C. R., Archibald, A. M., Ribeiro, A. H., Pedregosa, F., van Mulbregt, P., SciPy 1.0 Contributors, Vijaykumar, A., Bardelli, A. P., Rothberg, A., Hilboll, A., Kloeckner, A., Scopatz, A., Lee, A., Rokem, A., Woods, C. N., Fulton, C., Masson, C., Häggström, C., Fitzgerald, C., Nicholson, D. A., Hagen, D. R., Pasechnik, D. V., Olivetti, E., Martin, E., Wieser, E., Silva, F., Lenders, F., Wilhelm, F., Young, G., Price, G. A., Ingold, G.-L., Allen, G. E., Lee, G. R., Audren, H., Probst, I., Dietrich, J. P., Silterra, J., Webber, J. T., Slavic, J., Nothman, J., Buchner, J., Kulick, J., Schönberger, J. L., de Miranda Cardoso, J. V., Reimer, J., Harrington, J., Rodríguez, J. L. C., Nunez-Iglesias, J., Kuczynski, J., Tritz, K., Thoma, M., Newville, M., Kümmerer, M., Bolingbroke, M., Tartre, M., Pak, M., Smith, N. J., Nowaczyk, N., Shebanov, N., Pavlyk, O., Brodtkorb, P. A., Lee, P., McGibbon, R. T., Feldbauer, R., Lewis, S., Tygier, S., Sievert, S., Vigna, S., Peterson, S., More, S., Pudlik, T., Oshima, T., Pingel, T. J., Robitaille, T. P., Spura, T., Jones, T. R., Cera, T., Leslie, T., Zito, T., Krauss, T., Upadhyay, U., Halchenko, Y. O., and Vázquez-Baeza, Y.: SciPy 1.0: fundamental algorithms for scientific computing in Python, Nature Methods, 17, 261–272, https://doi.org/10.1038/s41592-019-0686-2, 2020.

Warscher, M., Hanzer, F., Becker, C., and Strasser, U.: Monitoring snow processes in the Ötztal Alps (Austria) and development of an open source snow model framework, in: EGU General Assembly Conference Abstracts, pp. EGU21–9101, Copernicus GmbH, https://doi.org/10.5194/egusphere-egu21-9101, 2021.

Winkler, M., Schellander, H., and Gruber, S.: Snow water equivalents exclusively from snow depths and their temporal changes: the ΔSNOW model, Hydrology and Earth System Sciences, 25, 1165–1187, https://doi.org/10.5194/hess-25-1165-2021, 2021.